

Investigations of the gas phase chemistry in a hot filament CVD reactor operating with $\text{CH}_4/\text{N}_2/\text{H}_2$ and $\text{CH}_4/\text{NH}_3/\text{H}_2$ gas mixtures

Yu.A. Mankelevich^{a,*}, N.V. Suetin^a, J.A. Smith^b, M.N.R. Ashfold^b

^aNuclear Physics Institute, Moscow State University, 119899 Moscow, Russia

^bSchool of Chemistry, University of Bristol, Cantock's Close, Bristol, BS8 1TS, UK

Abstract

We report a combination of experimental and theoretical studies of hot filament (HF) surface effects and the gas-phase chemistry prevailing in HF activated $\text{CH}_4/\text{N}_2/\text{H}_2$ and $\text{CH}_4/\text{NH}_3/\text{H}_2$ gas mixtures which provide some rationale for the observed low nitrogen doping levels in diamond films grown from such gas mixtures. The experimental studies involve use of resonance enhanced multiphoton ionisation (REMPI) to monitor relative H atom and CH_3 radical number densities in a HFCVD reactor as a function of filament temperature and N_2/CH_4 and NH_3/CH_4 gas mixing ratios. With NH_3 , contrary to N_2 , clear depletion of both H atom and CH_3 radical number densities are observed. The experimental observations are successfully reproduced using a previously developed 3-D model of HFCVD reactors. Three-dimensional (3-D) model calculations for C/H/N gas mixtures show significant N atom production due to successive 'H-shifting' reactions $\text{NH}_x + \text{H} \rightleftharpoons \text{NH}_{x-1} + \text{H}_2$ ($x=1-3$). N atom densities reach $5 \times 10^{13} \text{ cm}^{-3}$; their reaction with CH_3 radicals accounts for the observed depletion of the latter and results in eventual production of HCN. © 2002 Elsevier Science B.V. All rights reserved.

Keywords: Hot-filament CVD; H/C/N chemistry; Modelling; REMPI measurements

1. Introduction

Addition of small amounts of nitrogen to the typical hydrocarbon/ H_2 gas mixtures used for diamond chemical vapour deposition (CVD) in hot filament (HF) reactors can lead to significant changes in gas phase chemical composition, growth habits and deposition rates [1–6]. May and co-workers [7,8] investigated diamond CVD in a HF reactor using $\text{CH}_4/\text{NH}_3/\text{H}_2$, $\text{CH}_3\text{NH}_2/\text{H}_2$ and even HCN/H_2 gas mixtures. Diamond CVD was observed from $\text{CH}_4/\text{NH}_3/\text{H}_2$ feedstock gas mixtures, provided the input gas ratio $[\text{CH}_4]/[\text{NH}_3] \geq 1$, but the addition of NH_3 was found to reduce deposition rates due to substantial conversion of the input carbon to HCN, that acts as a sink for the carbon.

The combined programme of experiment and modelling described in this article seeks to provide a more detailed interpretation of the effects of controlled additions of nitrogen (in the form of N_2 and NH_3) to $\text{CH}_4/$

H_2 process gas mixtures in a HF-CVD reactor. The experimental part involves use of resonance enhanced multiphoton ionisation (REMPI) spectroscopy to provide spatially resolved measures of H atom and CH_3 radical number densities as a function of process conditions (e.g. feed-stock gas mixing ratio and the temperature, T_{fil} , of the Ta filament). The REMPI measurements are a natural extension of recent similar investigations for the case of diamond CVD when using CH_4/H_2 and $\text{C}_2\text{H}_2/\text{H}_2$ gas mixtures in the same HF-CVD reactor [9]. The results obtained are compared with the output of an existing 3-D model [10,11], specifically tailored to this HF-CVD reactor. The complete model comprises three blocks, describing (i) activation of the reactive mixture (i.e. gas heating and catalytic H atom production at the HF surface); (ii) gas-phase processes (heat and mass transfer, and chemical kinetics); and (iii) gas-surface processes at the substrate. The last of these sub-routines is not required for the present work as the experiments to be modelled were all performed without any substrate. The gas phase chemistry and thermochemical input is provided by the GRI-Mech 3.0 detailed reaction mechanism for C/H/

*Corresponding author. Tel.: +7-95-9394102; fax: +7-95-9390909.

E-mail address: yura@mics.msu.su (Y. Mankelevich).

N/O gas mixtures [12] (plus one additional reaction allowing destruction of the species H_2CN [13]). The set of conservation equations for mass, momentum, energy and species concentrations, together with appropriate initial and boundary conditions, thermal and caloric equations of state, are integrated numerically until attaining steady state conditions, thereby yielding spatial distributions of the gas temperature, the flow field, and the various species number densities. Comparisons between experiment and theory highlight the very different reactivities of N_2 and NH_3 in the present HF activated 1% CH_4/H_2 gas mixtures, reveal changes in filament surface conditions and unravel details of the gas phase chemistry prevailing when using $\text{CH}_4/\text{NH}_3/\text{H}_2$ process gas mixtures.

2. Operational characteristics of the hot filament upon adding nitrogen containing gases

Details of the HF-CVD reactor, and the REMPI detection schemes used for spatially resolved measurements of H atom and CH_3 radical number densities have been presented elsewhere [9,14] and are summarised only very briefly here.

The reactor is an evacuable stainless steel 6-way cross-equipped with quartz windows to allow passage of the focused probe laser beam. The temperature of the HF (250- μm -diameter Ta wire, seven turns, $\sim 3\text{-mm}$ coil diameter) is monitored with a two colour optical pyrometer (Land Infrared). The H_2 , CH_4 , NH_3 and/or N_2 feedstock gases are metered through separate mass flow controllers to maintain an overall flow rate of 100 sccm and total pressure of 20 torr. H atoms and CH_3 radicals are both detected by 2+1 REMPI using ultraviolet (UV) excitation wavelengths of 243.1 and ~ 333 nm, respectively. Relative number densities of H atoms (henceforth represented by $[\text{H}]$) and CH_3 radicals ($[\text{CH}_3]$) were measured as a function both of added $\text{NH}_3(\text{N}_2)$ and filament temperature, T_{fil} .

Addition of NH_3 to a 1% CH_4/H_2 gas mixture activated by a Ta HF was observed to cause a reduction in the T_{fil} value returned by the two colour optical pyrometer. Both the rate and the extent of the temperature drop, ΔT_{fil} (the difference between T_{fil} measured prior to any NH_3 addition and the asymptotic value found at long time, $t = \infty$) were found to increase with increasing NH_3 fraction ($\Delta T_{\text{fil}} \sim 58$ K for addition of 1% NH_3 and ~ 80 K for 5% added NH_3). Conversely, addition of 1% N_2 has a minimal effect on the observed T_{fil} . Each of the T_{fil} vs. t trends measured for the various NH_3 partial pressures is described well by a function of the form:

$$T_{\text{fil}}(t) - T_{\text{fil}}(t = \infty) = \Delta T_{\text{fil}} \exp(-t/\tau). \quad (1)$$

The observed time dependence of $T_{\text{fil}}(t)$ upon NH_3 addition can be rationalised by a simplified adsorption–

desorption (etching) kinetic scheme in which accommodation of a nitrogen containing gas phase species A on a surface site leads to N-termination. The time constant τ in such a model may be expressed as $\tau = (k_a[A] + k_d)^{-1}$, where $[A]$ is the number density of N containing species near the HF surface, and k_a and k_d are adsorption and desorption (etching) rate coefficients, respectively. Fitting the experimental data for addition of 1 and 5% NH_3 to a 1% CH_4 in H_2 gas mixture with $T_{\text{fil}} \sim 2473$ K yields values of $k_d \sim 0.01$ s^{-1} and $k_a[A] = 0.038$ and 0.157 s^{-1} , respectively. Eq. (1) is also found to provide a good description of the rate of the temperature recovery when the NH_3 flow is shut-off (and $[A] \rightarrow 0$).

Given knowledge of the input power supplied to the HF ($P_{\text{input}} = 87$ W for $T_{\text{fil}}(t=0) = 2473$ K and 1% CH_4/H_2 gas mixture) and estimates of the power expended on H_2 dissociation ($P_{\text{diss}} \sim 8$ W) and conductive losses ($P_{\text{cond}} \sim 10.7$ W) from the 3-D modelling, we can estimate the power radiated by the HF ($P_{\text{rad}} \sim 68$ W). This, in turn, allows estimation of the mean emissivity ε of the HF via Planck's radiation law. The emissivities so derived, $\varepsilon \sim 0.52$ and 0.61 for addition of 0 and 1% NH_3 , respectively, fall midway between literature values for the emissivity of TaC ($\varepsilon \sim 0.3$) and graphite ($\varepsilon \sim 0.9$) at $T \sim 2500$ K implying that, under these conditions, approximately half the filament surface has a graphitic overcoat. Since radiation is the main power loss mechanism in the present case, we propose that an increase in the emissivity of the HF surface upon NH_3 addition is responsible for the observed reduction of T_{fil} at constant P_{input} .

Falls in T_{fil} of comparable magnitude but quite different origin have been reported previously [14,15] in the case of carburised Ta filaments operating at high temperatures ($T_{\text{fil}} > 2800\text{--}3000$ K) and constant P_{input} when the hydrocarbon content in CH_4/H_2 gas mixtures is suddenly reduced. At first sight, the resulting fall in the number density of gas phase carbon species would be expected to reduce the extent of any graphitic overcoat on the HF surface, and thus lower the emissivity and cause T_{fil} to rise. However, the graphitic overcoat is much less efficient at catalysing H_2 dissociation than is a 'clean' TaC surface [14–16]. The observed drop in T_{fil} in such experiments is thus attributed to the increased fraction of P_{input} expended on surface catalysed H_2 dissociation. Such cannot be the case in the present experiments since (a) H_2 dissociation accounts for only a small fraction of P_{input} ; and (b) the REMPI measurements (see below) show the number density of gas phase H atoms to fall with added NH_3 even when T_{fil} is kept constant. Addition of 1% N_2 to a 1% CH_4/H_2 gas mixture causes negligible change to the measured H atom number, but adding 1% NH_3 results in an $\sim 40\%$ fall in $[\text{H}]$ for all filament temperatures in the range 2100–2700 K. As in previous studies of CH_4/H_2

mixtures [17], the near filament H atom number density was found to increase nearly exponentially throughout the T_{fil} range investigated, i.e. $[H] \sim \exp(-\Delta H_{\text{diss}}/RT_{\text{fil}})$, where $\Delta H_{\text{diss}} = 240 \pm 20 \text{ kJ mol}^{-1}$ is the enthalpy for H atom formation on the HF surface and R is the gas constant ($8.314 \text{ J mol}^{-1} \text{ K}^{-1}$).

3. Gas phase number densities and chemistry in H/C and H/C/N gas mixtures for different filament temperatures

Here we report results of 3-D model calculations for the Bristol HF-CVD reactor operating with different gas mixtures (1% CH_4/H_2 , 1% $\text{CH}_4/1\% \text{NH}_3/\text{H}_2$ and 1% $\text{CH}_4/1\% \text{N}_2/\text{H}_2$) and filament temperatures T_{fil} . Interpretation of the REMPI measurements of H and CH_3 relative number densities, and subsequent experimental data, builds on our previous modelling [11,18] of the gas phase chemistry occurring in activated CH_4/H_2 and $\text{C}_2\text{H}_2/\text{H}_2$ gas mixtures in the same HF-CVD reactor [9]. The reactor (with no substrate present) is represented in Cartesian co-ordinates with the z -axis parallel to the direction of feedstock gas flow (input \rightarrow output) and perpendicular to the filament, the centre axis of which is along y . x is orthogonal to both the filament axis and the direction of gas flow. The modelling considers the volume bounded by $x = \pm 16 \text{ mm}$, $y = \pm 18 \text{ mm}$ and $z = \pm 26 \text{ mm}$, with the point (0,0,0) defining the centre of the filament. $d=0$ corresponds to the point (0, 0, 1.5 mm). The points (0, 0, -26 mm) and (0, 0, +26 mm) define the gas inlet and outlet positions, where the gas temperature is set to $T_{\text{gas}} = 450 \text{ K}$. T_{gas} values at all other boundaries of the numerical grid, previously constrained also to be 450 K [11], were chosen more carefully so as to ensure that the temperature distribution far from the filament exhibits near spherical symmetry. Based on previous modelling [11,18], the temperature drop ($\Delta T = T_{\text{fil}} - T_{\text{inf}}$) between the filament surface and the immediate gas phase was varied slightly, from a value $\Delta T = 500 \text{ K}$ for $T_{\text{fil}} = 2700 \text{ K}$, through 475 K for $T_{\text{fil}} = 2500 \text{ K}$ and down to 350 K for $T_{\text{fil}} = 2200 \text{ K}$.

In the case of a 1% $\text{CH}_4/1\% \text{N}_2/\text{H}_2$ gas mixture, N_2 is seen to act as an essentially inert spectator, with a predicted fractional dissociation $[\text{N}]/[\text{N}_2] < 10^{-7}$ even at $T_{\text{gas}} \sim 2000 \text{ K}$ (i.e. in the immediate vicinity of the HF). Further simulations, in which this ratio was arbitrarily increased (such as might conceivably apply in the event of catalysed N_2 dissociation on the HF surface or, in the case of microwave activation, as a result of non-thermal plasma chemistry) indicate that the $[\text{N}]/[\text{N}_2]$ ratio would have to be at least two orders of magnitude to cause a measurable reduction in the measured $[\text{CH}_3]$.

To produce a realistic T_{fil} dependence for the H atom number densities we have adopted the experimentally observed exponential dependence for the model param-

eter Q that describes the net rate of H atom production per unit area of the HF surface, i.e.

$$Q(T_{\text{fil}}, \text{NH}_3) = Q_0(\text{NH}_3) \cdot \exp(-\Delta H_{\text{diss}}/RT_{\text{fil}}). \quad (2)$$

The REMPI measurements showed NH_3 addition to cause a reduction in $[H]$. This was accommodated in the model via use of a reduced Q parameter for the 1% $\text{CH}_4/1\% \text{NH}_3/\text{H}_2$ gas mixture, Q_0 (1% NH_3), and adopting a ratio Q_0 (1% NH_3)/ Q_0 (0% NH_3) ≈ 0.57 . Thus, we have just one parameter, Q_0 (0% NH_3) (henceforth denoted simply as Q_0), with which to match all REMPI measurements of $[\text{CH}_3]$ for different T_{fil} and gas mixtures.

In Fig. 1, CH_3 relative number densities measured 4 mm from the HF as a function of T_{fil} for a 1% CH_4/H_2 input gas mixture, with and without 1% added NH_3 , are compared with CH_3 concentrations calculated with $Q_0 = 3.6 \times 10^{24} \text{ cm}^{-2} \text{ s}^{-1}$. A range of Q_0 values were investigated, and the present value chosen so as to provide the local maximum of $[\text{CH}_3]$ at $T_{\text{fil}} \sim 2500 \text{ K}$. We note that this Q_0 is approximately one order of magnitude lower than those estimated in a previous investigation of the way in which the temperature of a Ta HF varied as a function of CH_4/H_2 input gas mixing ratio and the power supplied to the filament [15]. We also note, however, that in estimating the higher Q value Li et al. [15] assumed a value of 0.9 for the emissivity of their poisoned TaC filament — significantly higher than the real value ($\varepsilon \sim 0.5\text{--}0.6$) found for the conditions under study. Fig. 1 reproduces previous observations [19] of a smooth rise and saturation in $[\text{CH}_3]$ with increasing T_{fil} when using a standard 1% CH_4/H_2 mixture, and that addition of 1% NH_3 causes a marked decrease in $[\text{CH}_3]$, most notably at high T_{fil} .

Both trends are captured reasonably well by the model calculations and can be readily understood by inspecting the calculated temperature (and thus position) dependent number densities for the various participating species (Table 1) and inter-conversion rates (Table 2). Numerous previous studies have shown hydrocarbon based ‘H-shifting’ reactions of the form $\text{CH}_x + \text{H} \rightleftharpoons \text{CH}_{x-1} + \text{H}_2$ to be the dominant H atom loss mechanism in the hotter regions of HF activated CH_4/H_2 gas mixtures. Careful inspection of species number densities and the reaction rates presented in Tables 1 and 2 for $T_{\text{fil}} = 2600 \text{ K}$ and three different distances from the filament axis ($z = 2, 8$ and 16 mm) show that addition of NH_3 introduces a corresponding set of H-shifting reactions of the form $\text{NH}_x + \text{H} \rightleftharpoons \text{NH}_{x-1} + \text{H}_2$ which compete with the CH_x reaction sequence. Both sequences constitute significant loss processes for gas phase H atoms but both consumption rates are an order of magnitude slower than the deduced H atom production rate, Q .

The NH_x reaction sequence results in significant production of N atoms. Atomic nitrogen introduces additional purely gas phase CH_x loss processes, most

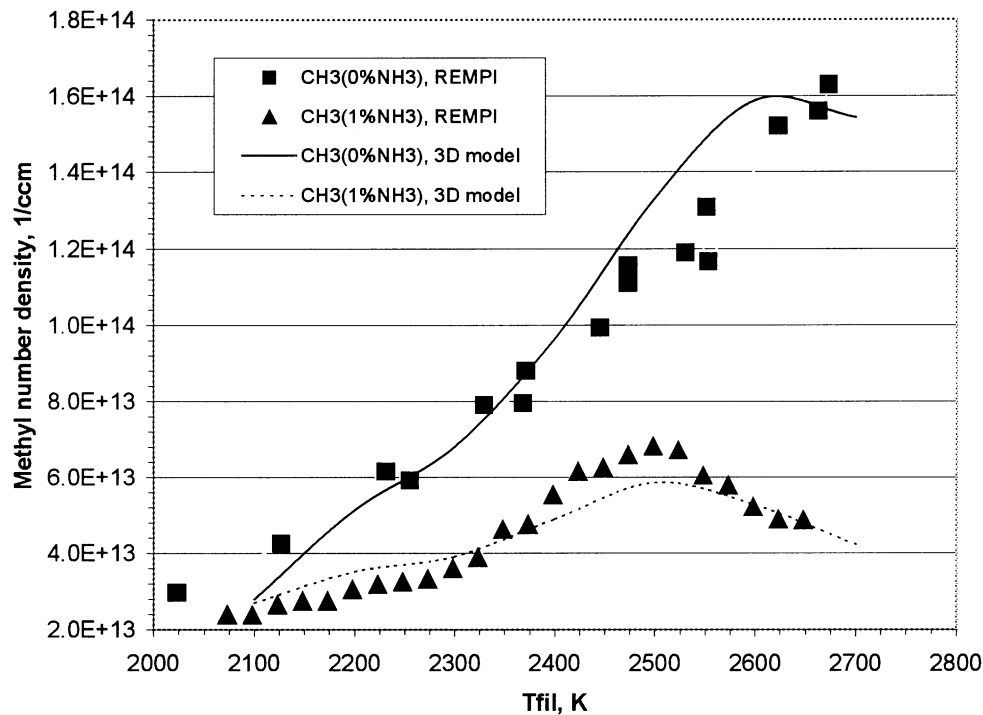


Fig. 1. Comparison between calculated methyl radical number densities and the relative CH_3 number densities determined experimentally, both at $d=4$ mm from the HF, plotted as a function of T_{fil} for a 1% CH_4/H_2 input gas mixture with and without 1% added NH_3 .

notably the irreversible transformation of CH_3 radicals to HCN (see Table 2). HCN acts as a sink for input NH_3 molecules also, as can be seen from Fig. 2. This figure shows calculated T_{fil} dependent number densities

Table 1

Calculated gas temperatures and species number densities [cm^{-3}] for a 1% $\text{CH}_4/1\%$ NH_3/H_2 input gas mixture at $z=2, 8$ and 16 mm below the centre of the HF

T_g/K	2100 K, $z=2$ mm	1217 K, $z=8$ mm	781 K, $z=16$ mm
H	3.26E+15	2.50E+15	1.98E+15
CH_3	4.31E+13	4.68E+13	4.41E+12
C_2H_2	5.56E+12	1.06E+13	1.16E+13
CH_2	1.62E+12	1.68E+11	3.23E+09
$\text{CH}_2(\text{s})$	1.18E+11	4.57E+09	6.49E+06
CH	1.98E+11	1.64E+10	3.20E+08
C	6.17E+11	9.48E+11	7.50E+11
C_2H	5.43E+09	4.22E+07	1.86E+05
C_2H_6	2.05E+09	3.06E+11	4.37E+11
C_2H_4	1.60E+11	5.49E+11	5.06E+11
C_2H_5	3.49E+09	5.33E+09	9.78E+08
C_2H_3	2.40E+10	1.24E+10	4.09E+10
N	1.84E+13	2.45E+13	2.70E+13
N_2	3.16E+12	6.55E+12	8.88E+12
NH	6.74E+12	1.41E+12	1.93E+11
NH_2	8.32E+12	3.82E+12	1.30E+12
CN	1.62E+11	5.23E+09	2.71E+07
HCN	1.72E+14	3.89E+14	4.75E+14
H_2CN	6.68E+10	2.82E+11	7.54E+10
NH_3	8.36E+13	2.93E+14	9.28E+14
CH_4	6.58E+13	2.70E+14	9.55E+14
H_2	8.80E+16	1.55E+17	2.43E+17

for the dominant hydrocarbons CH_4 and C_2H_2 in a 1% CH_4/H_2 input gas mixture, with and without 1% added NH_3 , along with the corresponding calculated NH_3 , HCN and N atom number densities in the latter case. The predicted T_{fil} dependences of $[\text{CH}_3]$, at a distance $d=4$ mm beneath the mid-point of the lower edge of the coiled filament (Fig. 1), show similar declines at higher T_{fil} for both H/C [19] and H/C/N mixtures. In both cases, input CH_4 molecules pass through a multi-step sequence of reactions en route to stable products C_2H_2 (in the case of H/C mixtures) and HCN (for H/C/N mixtures), thereby depleting the number densities of CH_x species both near the HF and in the surrounding volume extending out to distances where any substrate would normally be positioned in a diamond growth experiment. Given the critical role of methyl radicals in diamond growth in such HF-CVD reactors, the deduced reduction in $[\text{CH}_3]$ is wholly consistent with previous reports [7] of reduced diamond deposition rates when the input fraction of NH_3 begins to approach that of CH_4 . Finally, we note that the 3-D modelling predicts CN radical concentrations $< 10^{10} \text{ cm}^{-3}$ at all realistic filament–substrate distances. If, as has been suggested, N incorporation into a growing diamond film involves CN (instead of CH_3) addition to a vacant surface site, the deduced paucity of gas phase CN radicals in such HF activated mixtures could provide a ready explanation for the reported low N doping efficiencies [2,3,6].

Table 2

Calculated rates [$\text{cm}^{-3} \text{s}^{-1}$] of the more important direct R_i and reverse R_{-i} reactions involving nitrogen containing species at different distances z below the centre of the HF

i	Reactions	$R_i (z=2)$	$R_{-i} (z=2)$	$R_i (z=8)$	$R_{-i} (z=8)$	$R_i (z=16)$	$R_{-i} (z=16)$
1	$\text{NH}_3 + \text{H} \rightleftharpoons \text{NH}_2 + \text{H}_2$	2.17E+18	1.89E+18	2.76E+17	1.50E+17	2.43E+16	8.60E+15
2	$\text{NH}_2 + \text{H} \rightleftharpoons \text{NH} + \text{H}_2$	7.53E+17	5.98E+17	1.40E+17	1.16E+16	1.62E+16	5.81E+13
3	$\text{NH} + \text{H} \rightleftharpoons \text{N} + \text{H}_2$	1.08E+18	1.05E+18	1.64E+17	3.08E+16	1.64E+16	1.75E+14
4	$\text{CH}_3 + \text{N} \rightleftharpoons \text{H}_2\text{CN} + \text{H}$	7.01E+16	5.11E+12	1.14E+17	3.67E+10	1.27E+16	1.96E+06
5	$\text{CH}_3 + \text{N} \rightleftharpoons \text{HCN} + \text{H}_2$	1.57E+16	8.85E+08	2.12E+16	4.79E+00	2.11E+15	2.06E-11
6	$\text{CN} + \text{H}_2 \rightleftharpoons \text{HCN} + \text{H}$	5.70E+17	5.75E+17	5.70E+15	5.64E+15	9.31E+12	9.18E+12
7	$\text{H} + \text{HCN} + \text{M} \rightleftharpoons \text{H}_2\text{CN} + \text{M}$	1.07E+14	4.31E+16	1.51E+15	2.32E+16	6.76E+15	1.08E+14
8	$\text{H} + \text{H}_2\text{CN} \rightleftharpoons \text{HCN} + \text{H}_2$	2.82E+16	2.17E+13	9.12E+16	6.40E+07	1.93E+16	1.22E+00
9	$\text{H}_2\text{CN} + \text{N} \rightleftharpoons \text{N}_2 + \text{CH}_2$	1.12E+14	1.87E+06	5.83E+14	3.12E-01	1.57E+14	9.63E-11
10	$\text{NH} + \text{N} \rightleftharpoons \text{N}_2 + \text{H}$	3.10E+15	4.99E+03	8.63E+14	6.54E-08	1.30E+14	1.71E-22

4. Conclusions

Resonance enhanced multiphoton ionisation spectroscopy has been used to provide spatially resolved relative H atom and CH_3 radical number densities in a HF-CVD reactor operating with $\text{NH}_3/\text{CH}_4/\text{H}_2$ and $\text{N}_2/\text{CH}_4/\text{H}_2$ gas mixtures. These relative number density measurements are then placed on an absolute scale by recourse to realistic 3-D modelling of the chemistry prevailing in such HF activated gas mixtures. Experiment and theory agree in the view that N_2 is unreactive under the prevailing experimental conditions, whereas NH_3 additions have a major effect on the gas phase chemistry and composition. Specifically, addition of NH_3 introduces an additional sequence of H-shifting reactions result-

ing in the formation of N atoms with steady state concentrations approaching $5 \times 10^{13} \text{ cm}^{-3}$. These participate in reactions that convert CH_3 radicals, irreversibly, to HCN — thereby reducing the number density of free hydrocarbon species available to participate in diamond growth. The deduced reductions in $[\text{CH}_3]$ are entirely consistent with previous reports [7] that the rate of diamond deposition from $\text{CH}_4/\text{NH}_3/\text{H}_2$ gas mixtures is much reduced when the input fraction of NH_3 becomes comparable to that of CH_4 . Further support for the validity of the modelling of the gas-filament surface and pure gas phase chemistry is provided by very good agreement between the calculated spatial distribution of NH radical number densities in HF activated 1% $\text{CH}_4/5\% \text{ NH}_3/\text{H}_2$ gas mixtures and the absolute NH column

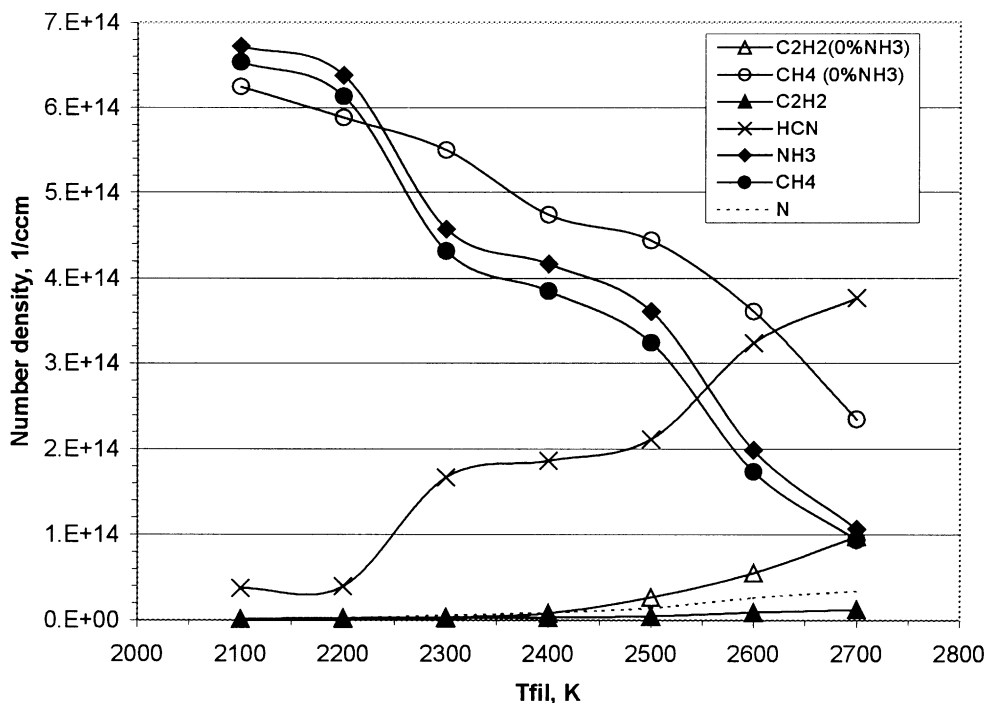


Fig. 2. Calculated species number densities at $d=4$ mm from the HF as a function of T_{fil} for 1% $\text{CH}_4/0\% \text{ NH}_3/\text{H}_2$ (open symbols) and 1% $\text{CH}_4/1\% \text{ NH}_3/\text{H}_2$ input gas mixtures.

densities in such mixtures obtained by cavity ring down spectroscopy [13]. Thus we arrive at a reasonably self-consistent picture of the gas phase transformations occurring in a HFCVD reactor operating at typical modest filament temperatures when NH_3 is added to a hydrocarbon/ H_2 gas mixture. NH_3 addition is also shown to induce surface modifications to the carburised HF, affecting both its emissivity and its ability to promote surface catalysed H_2 dissociation.

Acknowledgments

We are grateful to the EPSRC for equipment grants and for the award of a Senior Research fellowship (M.N.R.A.) and a studentship (J.A.S.), to the Royal Society for a Joint Project Grant to enable the Bristol–Moscow collaboration, and to NATO for the award of SFP grant N974354 (Y.A.M.).

References

- [1] J. Mort, M.A. Machonkin, K. Okumura, *Appl. Phys. Lett.* 59 (1991) 3148.
- [2] S. Jin, T.D. Moustakas, *Appl. Phys. Lett.* 63 (1993) 2354.
- [3] S. Jin, T.D. Moustakas, *Appl. Phys. Lett.* 65 (1994) 403.
- [4] C. Wild, R. Locher, P. Koidl, *Mater. Res. Soc.* 416 (1996) 75.
- [5] F.K. de Theije, J.J. Schermer, W.L.P. van Enckevort, *Diamond Relat. Mater.* 9 (2000) 1439.
- [6] K. Iakoubovskii, G.J. Adriaenssens, Y.K. Vohra, *Diamond Relat. Mater.* 10 (2001) 485.
- [7] P.W. May, P.R. Burridge, C.A. Rego, et al., *Diamond Relat. Mater.* 5 (1996) 354.
- [8] R.S. Tsang, C.A. Rego, P.W. May, M.N.R. Ashfold, K.N. Rosser, *Diamond Relat. Mater.* 6 (1997) 247.
- [9] J.A. Smith, E. Cameron, M.N.R. Ashfold, Y.A. Mankelevich, N.V. Suetin, *Diamond Relat. Mater.* 10 (2001) 358.
- [10] Yu.A. Mankelevich, A.T. Rakhimov, N.V. Suetin, *Diamond Relat. Mater.* 7 (1998) 1133.
- [11] Yu.A. Mankelevich, N.V. Suetin, M.N.R. Ashfold, J.A. Smith, E. Cameron, *Diamond Relat. Mater.* 10 (2001) 364.
- [12] G.P. Smith, D.M. Golden, M. Frenklach et al., http://www.me.berkeley.edu/gri_mech/
- [13] J.A. Smith, J.B. Wills, H.S. Moores et al., *J. Appl. Phys.* (submitted).
- [14] D. Morel, W. Hänni, *Diamond Relat. Mater.* 7 (1998) 826.
- [15] D.M. Li, R. Hernberg, T. Mäntylä, *Diamond Relat. Mater.* 7 (1998) 1709.
- [16] H.F. Winters, H. Seki, R.R. Rye, M.E. Coltrin, *J. Appl. Phys.* 76 (1994) 1228.
- [17] S.A. Redman, C. Chung, K.N. Rosser, M.N.R. Ashfold, *Phys. Chem. Chem. Phys.* 1 (1999) 1415.
- [18] M.N.R. Ashfold, P.W. May, J.R. Petherbridge, et al., *Phys. Chem. Chem. Phys.* 3 (2001) 3471.
- [19] E.J. Corat, D.G. Goodwin, *J. Appl. Phys.* 74 (1993) 2021.